Cod glycopeptide with picomolar affinity to galectin-3 suppresses T-cell apoptosis and prostate cancer metastasis

Prasun Guha[a,b], Engin Kaptan[a,b], Gargi Bandyopadhyaya[a,b], Sabina Kaczanowska[c], Eduardo Davila[c,d], Keyata Thompson[e], Stuart S. Martin[d,e], Dhananjaya V. Kalvakolanu[d,f], Gerardo R. Vasta[b,f], and Hafiz Ahmed[a,b,d,1]

[a]Department of Biochemistry and Molecular Biology, [b]Institute of Marine and Environmental Technology, [c]Department of Otorhinolaryngology, [d]University of Maryland Greenebaum Cancer Center, and Departments of [e]Physiology and [f]Microbiology and Immunology, University of Maryland School of Medicine, Baltimore, MD 21201

Edited by Chi-Huey Wong, Academia Sinica, Taipei, Taiwan, and approved February 19, 2013 (received for review February 14, 2012)

Cancer metastasis and immune suppression are critical issues in cancer therapy. Here, we show that a β-galactoside–binding lectin [galectin-3 (gal3)] that recognizes the Thomsen-Friedenreich disaccharide (TFD, Galβ1,3GalNAc) present on the surface of most cancer cells is involved in promoting angiogenesis, tumor-endothelial cell adhesion, and metastasis of prostate cancer cells, as well as evading immune surveillance through killing of activated T cells. To block gal3-mediated interactions, we purified a glycopeptide from cod (designated TFD_{100}) that binds gal3 with picomolar affinity. TFD_{100} blocks gal3-mediated angiogenesis, tumor-endothelial cell interactions, and metastasis of prostate cancer cells in mice at nanomolar levels. Moreover, apoptosis of activated T cells induced by either recombinant gal3 or prostate cancer patient serum-associated gal3 was inhibited at nanomolar concentration of TFD_{100}. Because the gal3–TFD interaction is a key factor driving metastasis in most epithelial cancers, this high-affinity TFD_{100} should be a promising anti-metastatic agent for the treatment of various cancers, including prostate adenocarcinoma.

antifreeze glycoprotein | PC3-luciferase cells | galectin-3 knockout PC3-luciferase cells | TF antigen | surface plasmon resonance

Tumor–endothelial interaction and angiogenesis are considered key steps before cancer metastasis (1), and disruption of such interactions may effectively prevent metastasis. It is now well established that carcinomas express Thomsen-Friedenreich (TF) antigen (Galβ1–3GalNAcα1-Ser/Thr) (2). The TF antigen (also known as CD176), present in the core I structure of mucin-type *O*-linked glycan, is generally masked by sialic acid in normal cells, but is exposed or nonsialylated in malignant epithelia (2). Increased surface expression of TF antigen is associated with a poorer prognosis in many cancers, suggesting that the TF antigen is somehow involved in cancer progression and metastasis (2). Cancer metastasis involves a series of steps including angiogenesis, detachment of a metastatic cell from the primary tumor, intravasation, evasion of host defense, arrest at a distant site, attachment, extravasation, dormant survival, and establishment of new growth. During extravasation, cancer cells bind to endothelial cells through protein–carbohydrate interactions and penetrate through the endothelium and basement membrane (1). Galectin-3 (gal3), one of the 15 members of a β-galactoside–binding lectin family, promotes tumor-endothelial cell adhesion. Gal3 expressed by the capillary endothelium participates in docking of cancer cells by specifically interacting with the TF disaccharide (TFD, Galβ1–3GalNAc) present on their surface (3). Further, tumor-secreted or circulating gal3 indirectly promotes tumor-endothelial cell interactions by binding to tumor-associated TFD-expressing mucin1 (MUC1) (4). This gal3-MUC1 binding polarizes MUC1, which otherwise shields smaller cell adhesion molecules, allowing epithelial–endothelial interactions via ligands such as E-selectin and CD44H (4). The circulating gal3 also mediates homotypic adhesion of cancer cells by binding to the surface TFD (5, 6), although other interactions may be involved. Besides gal3-mediated tumor–endothelial interactions described above, intracellular gal3 enhances mitochondrial stability and inhibits apoptosis in prostate cancer (PCa) cells in presence of certain chemotherapeutics (7). In addition to both intracellular and extracellular functions (8), tumor-secreted gal3 induces apoptosis of infiltrating T cells, thus acting as a double-edged sword to evade immune surveillance during tumor progression (9, 10). Based on these observations, we hypothesize that exogenous TFD would block gal3-mediated homotypic aggregation and tumor cell–endothelial interactions to prevent metastasis. Further, TFD would also block gal3-mediated T-cell apoptosis to facilitate anti-tumor immune response.

Among natural sources of TF antigen, polar fish such as the Antarctic notothenioid *Trematomus nicolai* and northern cods [Atlantic cod (*Gadus morhua*), Greenland cod (*Gadus ogac*), and Pacific cod (*Gadus macrocephalus*)] express abundant antifreeze glycoproteins (AFGP) that are rich in TFD and provide protection from freezing (11). Fish AFGPs are usually composed of several repeats of tripeptide of alanine-alanine-threonine in which the last triad is glycosidically linked to TFD (11). To explore the potential antitumor properties of a TFD-containing natural product that could be taken as food supplement, we purified a TFD-containing glycopeptide of molecular mass 100 kDa (designated TFD_{100}) from the Pacific cod by affinity chromatography and gel permeation chromatography. TFD_{100} inhibited in vitro adhesion of androgen-independent prostate cancer cells PC3 to endothelial cells, angiogenesis, and gal3-mediated T-cell apoptosis and also prevented PC3-induced metastasis in mice. This TFD-containing bioactive natural product from an edible species has applications in cancer therapeutics, particularly PCa.

Results

Purification and Characterization of TFD_{100}. A preliminary analysis of size-based fractionation of commercial cod fish antifreeze glycoproteins (AFGP; A/F Proteins) resulted five fractions, of which only three fractions (Fr1–3) had TFD (Galβ1,3GalNAc) as confirmed by binding of peanut lectin (PNA) (Table S1 and Fig. S1*A*). Among the various AFGP fractions tested, Fr1 was very active (Fig. S1*B*, see also Table S1) as an inhibitor of the binding of gal3 to asialofetuin. Based on these results, the followup purification procedure was aimed to identify the most active fraction. For this purpose, either commercial AFGP (cod glycoproteins) or crude extract of whole cod was subjected to affinity purification followed by gel permeation chromatography. Gel permeation chromatography of the affinity purified TFD-containing glycopeptides

Author contributions: P.G. and H.A. designed research; P.G., E.K., G.B., and H.A. performed research; S.K., E.D., K.T., S.S.M., D.V.K., and G.R.V. contributed new reagents/analytic tools; P.G., E.K., G.B., and H.A. analyzed data; and H.A. wrote the paper.

Conflict of interest statement: The US Patent entitled "Methods of use for a natural Thomsen-Friedenreich disaccharide compound" has been filed in March 2012.

This article is a PNAS Direct Submission.

[1]To whom correspondence should be addressed. E-mail: hahmed@som.umaryland.edu.

This article contains supporting information online at www.pnas.org/lookup/suppl/doi:10.1073/pnas.1202653110/-/DCSupplemental.

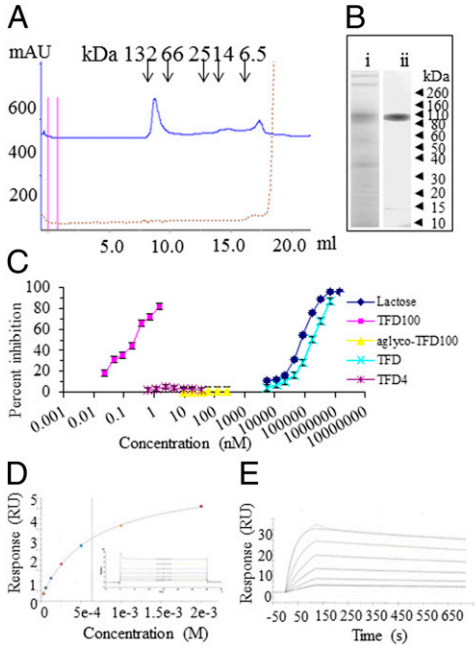

Fig. 1. Purification and characterization of TFD_{100}. (*A*) Separation of affinity-purified TFD-containing glycopeptides on a Superdex 75 10/300 GL column calibrated with BSA (dimer 132 kDa and monomer 66 kDa), chymotripsinogen (25 kDa), ribonuclease A (14 kDa), and aprotinin (6.5 kDa). (*B*) SDS/PAGE under reducing condition on 4–12% Bis-Tris gels followed by silver staining: (i) Crude AFGP (10 μg); (ii) TFD_{100} (5 μg). (*C*) Inhibition of gal3 binding to asialofetuin. Inhibition of gal3 binding to asialofetuin by various concentrations of compounds. (*D* and *E*) Surface plasmon resonance assay on Biacore. (*D*) TFD (Galβ1,3GalNAc) was measured from 31 μM to 1,000 μM, and the dissociation constant (K_D) was determined to be 6.36^{e-4} M or 636 μM. (*E*) TFD_{100} was measured from 0.312 nM to 10 nM, and the K_D was determined to be 9.677^{e-11} M or 97 pM. The full kinetic analysis results are as follows: $k_a = 3.105^{e+6}$ (1/ms); $k_d = 3.004^{e-4}$ (1/s); $K_D = 9.677^{e-11}$ M; $R_{max} = 31$ (resonance units; RU); Tc = 2.26^{e+18}; $\chi^2 = 0.112$ (RU^2); U value = 2.

yielded two major peaks corresponding to ∼100 kDa (designated as TFD_{100}) and 4 kDa, respectively (Fig. 1*A*). The 100-kDa peak (TFD_{100}) displayed a dramatically higher inhibitory activity than the 4-kDa peak on gal3 binding (Fig. 1*C*). On SDS/PAGE under reducing conditions, TFD_{100} migrated as a single band with an apparent M_r of ∼100 kDa (Fig. 1*B, ii*). Considering the molar concentration, the TFD_{100} (I_{50} at 0.25 nM) was 800,000-fold active in inhibiting gal3 binding compared with free TFD (I_{50} at 200 μM), whereas the 4-kDa peak was inactive even at 37 nM (Fig. 1*C*). The importance of *O*-glycan in gal3–TFD_{100} interaction was confirmed with an alkaline-treated TFD_{100}, which was inactive up to highest concentration (250 nM) tested (Fig. 1*C*).

The binding kinetics and affinity of TFD_{100} to gal3 was characterized by surface plasmon resonance analysis. The TFD_{100} binding interaction with gal3 was compared with the gal3 binding to lactose, *N*-acetyllactosamine, and TFD (Gal3β1,3GalNAc) to assess whether differences in the speed and strength of binding could be shown. Lactose (K_D 110 μM) (Fig. S2*A*), *N*-acetyllactosamine (K_D 25 μM) (Fig. S2*B*), and TFD (K_D 636 μM) exhibited extremely fast association and dissociation rates that were beyond the limits of resolution for reliable kinetic analysis (Fig. 1*D*). Steady-state affinity analysis provided a means of comparing the equilibrium dissociation constants to that of TFD_{100} binding (Fig. 1*E*). Surface plasmon resonance analysis revealed that TFD_{100} bound to gal3 with significantly higher affinity compared with all other carbohydrates measured. The interaction of TFD_{100} with gal3 exhibited an affinity that was stronger than the other carbohydrates by ∼6 orders of magnitude (K_D 97 pM). This difference in affinity was primarily driven by a considerably slower dissociation rate for TFD_{100}, which is indicative of a very stable complex. The measured dissociation rate of 3^{e-4} per s is equivalent to a half-life for the complex of 38.5 min. This binding is in contrast to the interactions with the other carbohydrates that had half-lives that were less than 1 s.

Because gal4 and gal9 are known to bind TFD (12, 13), we investigated relative binding activity of TFD_{100} toward gal4 and N-terminal of gal9 in a solid phase assay. The interaction of asialofetuin with gal4 (I_{50} 1.2 nM) and N-terminal of gal9 (I_{50} 1.5 nM) was five and six times, respectively, less compared with gal3 (I_{50} 0.25 nM) (Table S2).

TFD_{100} Inhibits Angiogenesis. Because angiogenesis is an essential step of metastasis, TFD_{100} was investigated for its potential antiangiogenic properties. Studies were carried out in both in vitro on human umbilical vein endothelial cells (HUVECs) and in vivo on C57BL/6 black mice. When grown in vitro by using selected media, HUVECs rapidly align and form hollow tube-like structures (Fig. 2*A*). Interestingly, tube formation was enhanced by ∼25% in presence of recombinant gal3 (5 μM) (Fig. 2 *A* and *B*) as assessed by tube branching. The data were significant (two-tailed *P* value is 0.021). The tube formation was inhibited by 70–75% with 3.5 nM TFD_{100} (Fig. 2 *A* and *B*). Because lactose is a known common inhibitor of galectins, we used 50 μM lactose as a positive control, which also inhibited tube formation by 70–75% (Fig. 2 *A* and *B*). The role of gal3 in tube formation was confirmed as down-regulation of gal3 reduced tube formation by approximately 55% (Fig. 2*C*). The participation of gal4 and gal9 in tube formation was also evident as treatment of HUVECs with respective siRNAs reduced tube formation by approximately 60% (Fig. 2*C*). The addition of TFD_{100} to HUVECs treated with either gal4 siRNA or gal9 siRNA, but not with gal3 siRNA, further reduced tube formation by ∼50%, suggesting the affinity of TFD_{100} affinity was directed to endogenous gal3 (Fig. 2*C*).

To assess in vivo the antiangiogenic activity of TFD_{100}, a VEGF-induced formation matrigel plug assay in the absence or presence of gal3 and TFD_{100} was performed in mice. Although VEGF-induced formation of blood vessels was further enhanced by 33% ($P < 0.05$) in the presence of 0.03 μM external gal3, TFD_{100} (2 nM) inhibited this effect with VEGF alone by 83% ($P < 0.01$) and by 67% ($P < 0.01$) in the presence of gal3 (Fig. 3).

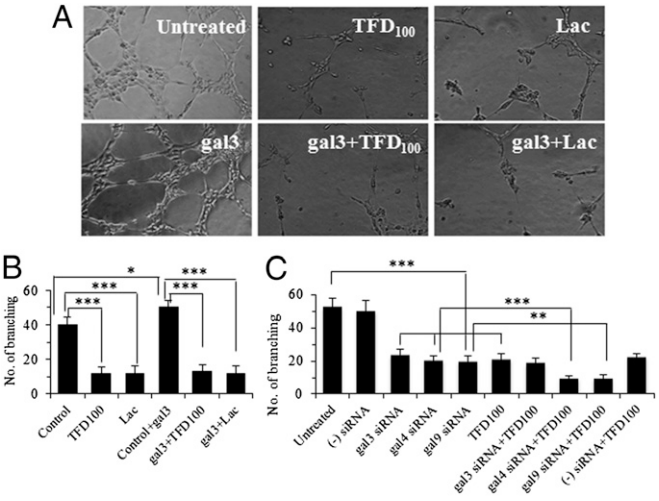

Fig. 2. In vitro angiogenesis. (*A*) Angiogenesis of HUVECs in the absence or presence of external gal3 and inhibition of angiogenesis with 3.5 nM TFD_{100} or 50 μM lactose. (*B*) Quantitation of angiogenesis as measured by number of capillary tube branch point. (*C*) Quantitation of capillary tube formation by HUVECs after treating with various siRNAs in the presence or absence of TFD_{100}. The data in *B* and *C* are shown as the means ± SD from three determinations. ***$P < 0.001$; **$P < 0.01$; *$P < 0.05$; ANOVA.

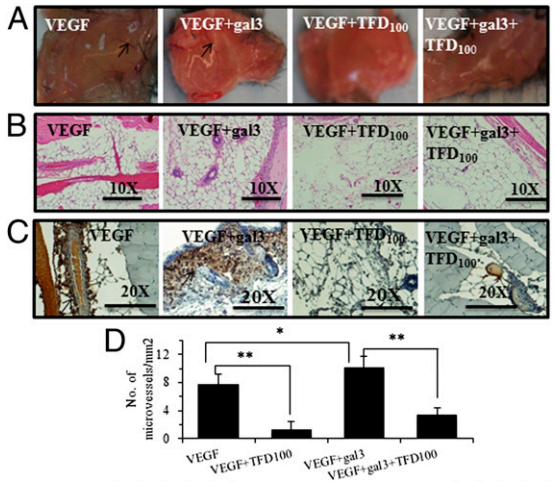

Fig. 3. In vivo angiogenesis. A mixture of matrigel and VEGF in the absence or presence of gal3 and TFD_{100} was administered in each mouse (strain C57BL/6 black) under skin at the abdomen. After a week, mice were euthanized and matrigel plugs were removed (*A*) and stained with hematoxylin and eosin (*B*), and anti-CD31 antibodies (*C*). Arrows show blood vessels. (*D*) Quantitation of microvessels. The data are shown as the means ± SD from three determinations. $^{**}P < 0.01$; $^{*}P < 0.05$; ANOVA.

TFD_{100} Inhibits Tumor–Endothelial Cell Interactions. To examine the in vivo relevance of the in vitro antiangiogenic activity of TFD_{100}, we first investigated expression of TFD in normal, benign prostatic hyperplasia (BPH), and various stages of PCa. Expression of gal3 in normal and PCa tissues was also investigated by us and others (14, 15). Gal3 was found strongly expressed in normal and BPH, but its expression was progressively decreased in higher stages (ref. 15, see also Fig. S3*A*). The data were statistically significant among groups, except for stage III–IV comparison (15).

Expression of TFD in normal and PCa tissues was examined by staining with anti-TFD antibody or PNA-FITC. In both cases, strong expression of TFD was observed in stage II–IV PCa (Fig. S3 *B* and *C*). The data were statistically significant compared with normal (Fig. S4 *A* and *B*).

For in vitro investigation of tumor–endothelial cell interactions, either HUVECs or labeled PC3 cells (with calcein) were preincubated with various reagents, washed, and the labeled PC3 cells were allowed to interact with a monolayer of HUVECs. As a first step, expression of gal3 and TFD was investigated in both PC3 cells and HUVECs. PC3 cells expressed both gal3 (Fig. S5*A*) and TFD (Fig. S5*B*) on their surfaces as demonstrated by binding with anti-gal3 antibody and PNA, respectively, by flow cytometry. However, HUVECs express only gal3 (Fig. S5*C*), but not TFD (Fig. S5*D*) on their surfaces. The absence of TFD in HUVECs was confirmed with glycan differentiation analysis because PNA failed to bind with the HUVEC extract (Fig. S5 *E, ii*). The expression of gal3 in PC3 cells and HUVECs is consistent with other studies (14, 15).

In the assessment of the effect of TFD_{100} on tumor–endothelial cell interactions, the fluorescently labeled PC3 cells readily bound to HUVEC monolayer and the binding was inhibited by 42% when the HUVECs were pretreated with 3.5 nM TFD_{100} (Fig. 4*A*). The PC3–HUVEC interaction was inhibited by 34% when gal3 was knocked down in HUVECs by using siRNA. The inhibition remained almost unchanged (39%) when the HUVECs were treated with both gal3 siRNA and TFD_{100}. To investigate other receptors that might be involved in PC3–HUVEC interactions, HUVECs were preincubated with antibodies against integrin, MUC1, and VEGFR1 and 17–36% inhibition of PC3–HUVEC interactions was observed. To investigate whether TFD_{100} could inhibit interactions between PC3 and activated endothelial cells, HUVECs were treated with tumor necrosis factor (TNF) and tumor–endothelial cell interactions were performed in the presence of TFD_{100}. As shown in Fig. 4*B*, TFD_{100} inhibited interactions of PC3 equally (approximately 39%) well to either nonactivated or activated HUVECs.

When PC3 cells were preincubated with 3.5 nM TFD_{100}, tumor–endothelial cell interactions were inhibited by 33% (Fig. 4*C*). No inhibition of PC3–HUVEC interaction was observed when PC3 cells were treated with 50 μg of TFD negative fraction 4 (Fig. 4*C* and Table S1). Similar to HUVECs, the inhibition of PC3–HUVEC interaction was more or less same when gal3 expression was knocked down in PC3 by using RNAi, or when combined with the TFD_{100}. Moreover, treatment of PC3 with specific antibodies (such as integrin, MUC1, and VEGFR1) showed inhibition of PC3–HUVEC interactions (Fig. 4*C*). Because gal4 and gal9 are known to be involved in tumor–endothelial cell interactions, PC3 cells were treated with siRNAs against these galectins and the treated cells were allowed to interact with the HUVECs. Down-regulation of these galectins resulted in 11–19% inhibition of PC3–HUVEC interactions (Fig. 4*D*). However, the inhibition of PC3–HUVEC interactions was increased to 37–40%, when TFD_{100} was combined with either gal4 or gal9 siRNA (Fig. 4*D*). Taken together, results suggest that both gal3-dependent and gal3-independent interactions are involved in PC3–HUVEC interactions.

Because gal3 is expressed in both PC3 cells and HUVECs, we knocked down gal3 expression in both cells by using RNAi and performed tumor–endothelial cell interaction. Interestingly, gal3 siRNA treatment of both cells resulted in inhibition (41%) as good as single treatment to either cell (Fig. 4*E*). Similarly, treatment of both cells with TFD_{100} (3.5 nM) inhibited tumor–endothelial interaction by 35%. These results further corroborate that other gal3-independent interactions are involved between PC3 cells and HUVECs.

Gal3-Induced Apoptosis of Human T Cells (MOLT-4 and Jurkat) and Its Inhibition with TFD_{100}. Because most human cancer cells are successful in blocking or evading the host–immune response, we next examined whether TFD_{100} could protect T cells from tumor-induced apoptosis. The ability of TFD_{100} to inhibit gal3-mediated apoptosis of T cells was first examined in human T-cell lines. As shown in phase contrast microscopy, the purified recombinant gal3 (5 μM) induced apoptosis of MOLT-4 cells through aggregation (Fig. S6*A*). Annexin V binding analyses showed that ~50%

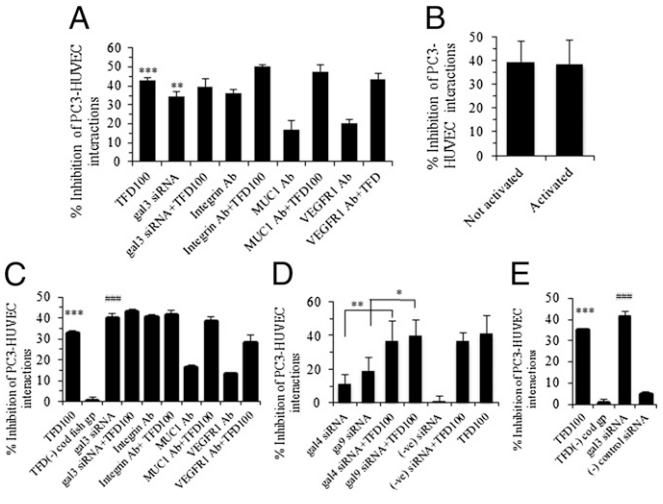

Fig. 4. PC3–HUVEC interactions. (*A*) Quantitation of bound PC3 cells on HUVECs pretreated with various reagents. (*B*) Inhibition of PC3 cell adhesion to activated and nonactivated HUVECs with TFD_{100} (3.5 nM). (*C* and *D*) Quantitation of bound PC3 cells pretreated with various reagents on HUVECs. (*E*) Both PC3 cells and HUVECs were pretreated with TFD_{100} (3.5 nM), and siRNA and PC3 cell adhesion to HUVECs was performed. All data are shown as the means ± SD from three determinations. $^{***}P < 0.001$; $^{\#\#\#}P < 0.001$; $^{**}P < 0.01$; $^{*}P < 0.05$; ANOVA. In *A*, *C*, and *E*, data showing significance are against untreated PC3–HUVEC control interactions.

of MOLT-4 cells underwent apoptosis in presence of gal3. This apoptosis was inhibited by 34% in presence of 3.5 nM TFD_{100} or by ~20% with 50 μM lactose (Fig. S6*A*). Like MOLT-4, Jurkat cells underwent gal3 (5 μM)-mediated apoptosis (~34%) but was inhibited (~63%) by 3.5 nM of TFD_{100} (Fig. S6*B*). The gal3-mediated apoptosis was also suppressed by a known inhibitor, lactose (~30% inhibition with 50 μM lactose) (Fig. S6*B*). In contrast, glucose (noninhibitor of gal3) did not protect gal3-mediated apoptosis of Jurkat cells, suggesting the gal3-mediated cell death was carbohydrate dependent. To determine the lowest concentration of gal3 required to induce T-cell death, Jurkat cells were incubated with gal3 (10 nM to 10 μM) and cell death was assessed. A dose-dependent cell death was observed with the lowest concentration of gal3 (10 nM) causing ~8% cell death (Fig. S6*C*). Gal3-mediated apoptosis of T cells was confirmed by TUNEL assay on Jurkat cells. On TUNEL assay, gal3 induced T-cell apoptosis, which was blocked by lactose (Fig. S6*D*).

Induction of Apoptosis of Tumor-Specific $CD8^+$ T Cells by Recombinant, Serum-Associated, and Tumor Cell-Associated gal3 and Its Inhibition with TFD_{100}. To investigate whether tumor-associated gal3 could induce tumor-specific $CD8^+$ T cells, we used B16 melanoma-specific T-cell transgenic D90.1 $CD8^+$ T cells (pmel T cells) as a model system (16). Following harvest of tumor-specific T cells from mouse spleen, a portion of cells was activated with a peptide, allowed to proliferate in presence of IL-2, and investigated for apoptosis with gal3 (recombinant, tumor cell-associated, or patient serum-associated). Nonactivated $CD8^+$ T cells at day 2 were also investigated for gal3-mediated apoptosis. Nonactivated $CD8^+$ T cells were insensitive to recombinant gal3 even up to 15 μM (~22% cell death in $CD8^+$ cells alone or in the presence of gal3) (Fig. 5 *B–D*). In contrast to the nonactivated T cells above, apoptosis of activated $CD8^+CD25^+$ T cells was induced with 5 μM recombinant gal3 (56% apoptosis, $P < 0.001$) (Fig. 5 *F* and *H*). Gal3-mediated apoptosis of activated T cells was inhibited by 81% ($P < 0.001$) with 3.5 nM TFD_{100} and by 48% ($P < 0.01$) with 50 μM lactose (Fig. 5 *G* and *H*).

To investigate whether tumor-associated gal3 can induce apoptosis of activated T cells, activated tumor-specific $CD8^+$ T cells were incubated on a monolayer of B16 cells for approximately 24 h and apoptosis was measured. B16 melanoma cells were first confirmed to express gal3 on the surface (Fig. 5*I*). Tumor cell (B16)-associated gal3 induced apoptosis of activated $CD8^+CD25^+$ T cells by 10% (Fig. 5*J*). However, TFD_{100} (3.5 nM) inhibited apoptosis of those activated T cells by 68% ($P < 0.05$) (Fig. 5*J*). B16 tumor cells treated with gal3 siRNA, but not with negative control siRNA, showed similar inhibition (68%, $P < 0.05$) of T-cell apoptosis (Fig. 5*J*).

To investigate whether serum gal3 from a cancer patient can induce apoptosis of activated $CD8^+CD25^+$ T cells, gal3-containing or gal3-depleted PCa patient serum was mixed with tumor-specific activated $CD8^+CD25^+$ T cells and apoptosis was measured. The PCa patient sera were found to contain a significantly higher amount of gal3 (16–240 ng/mL, $P < 0.001$) compared with normal or BPH serum (1.6 ng/mL) as quantitated by immunoassay (Table S3 and Fig. S6*E*). The patient sera induced apoptosis of activated $CD8^+CD25^+$ T cells by 73–83% ($P < 0.001$ compared with that induced by normal or BPH serum) (Fig. 5*K*). In some sera, TFD_{100} (1 nM) was added to inhibit gal3-mediated apoptosis of the activated T cells. All gal3-depleted patient sera, except two (P17 and P22), showed significant (more than 60%, $P < 0.001$ and $P < 0.05$) reduction of apoptosis compared with the corresponding parent serum (Fig. 5*K*). Taken together, results support the role of serum gal3 in induction of apoptosis of activated T cells.

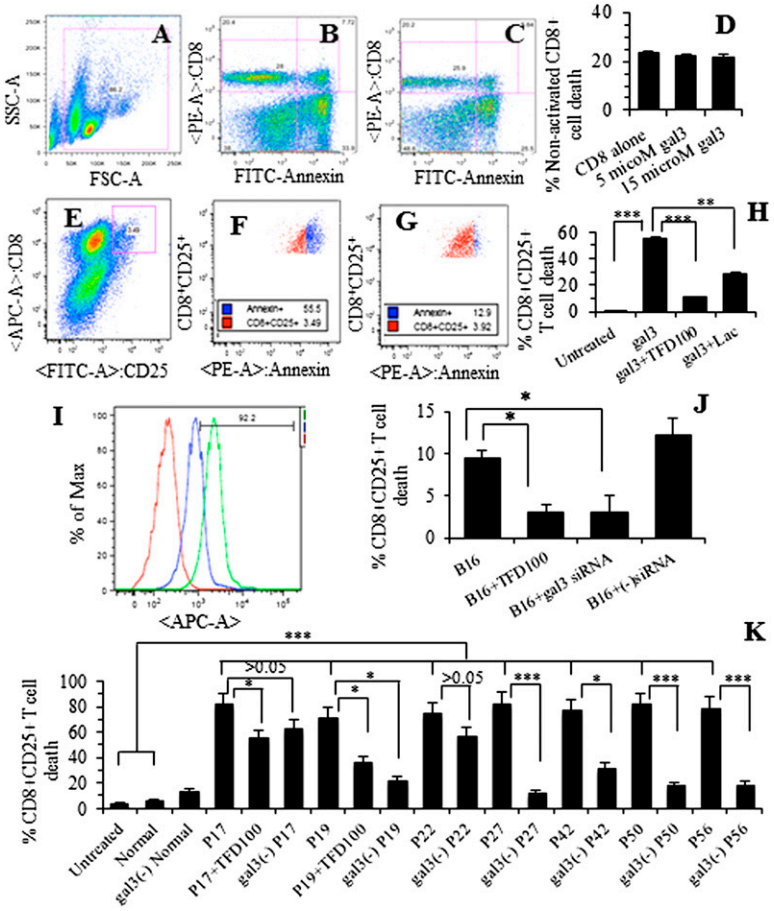

Fig. 5. Apoptosis of nonactivated $CD8^+$ (*A–D*) and activated (*E–G*) $CD8^+CD25^+$ T cells. (*A*) Gating of nonactivated pmel T cells. (*B*) pmel T cells alone. (*C*) pmel T cells with gal3 (15 μM). (*D*) Quantitation showing percent of nonactivated T cells. (*E*) Gating of pmel activated $CD8^+CD25^+$ T cells (shown in red square). (*F*) Representative cytogram showing apoptosis of pmel activated $CD8^+CD25^+$ T cells with gal3 (5 μM). (*G*) Representative cytogram showing apoptosis of pmel activated $CD8^+CD25^+$ T cells with gal3 plus TFD_{100} (3.5 nM). (*H*) Quantitation showing percent of activated $CD8^+CD25^+$ T cells. (*I*) Overlay cytograms showing expression of gal3 on B16 melanoma cell surface (red, unstained cells, mean fluorescence unit 214; green, with gal3 Ab, mfu 2832; and blue, with preimmune IgG, mfu 1005. (*J*) B16 cell-associated apoptosis of pmel activated $CD8^+CD25^+$ T cells. Quantitation of B16-mediated apoptosis of pmel activated $CD8^+CD25^+$ T cells in the presence of 3.5 nM TFD_{100} or gal3 siRNA. (*K*) Apoptosis of activated $CD8^+CD25^+$ T cells with gal3-containing or gal3-depleted sera from normal and PCa patients as assessed by annexin V binding. All data are shown as the means ± SD from three determinations. ***$P < 0.001$; **$P < 0.01$; *$P < 0.05$; ANOVA.

Role of gal3 in PCa Metastasis and Blocking of Metastasis with TFD_{100}. Because PC3 cells express and secrete gal3, we next investigated the effect of TFD_{100} on formation of metastases. To further corroborate the role of gal3 in the formation of metastasis, we stably transfected PC3-Luc cells (PC3 cells expressing a luciferase reporter) with gal3 shRNA to prepare gal3 knockout ($gal3^{-/-}$) PC3-Luc cells (Fig. 6*B*). However, expression of gal4 and gal9 in the gal3 knockout PC3 cells remained unchanged (Fig. 6*B*). Nude mice were administered with either gal3-containing wild-type PC3-Luc cells or $gal3^{-/-}$ PC3-Luc cells (10 mice for each group), and tumor growth and motility in vivo were monitored by using the Xenogen IVIS system for a period of 5 wk. Half of each group (5 mice) received TFD_{100} twice a week, whereas the other half received PBS (vehicle). Live imaging of each mouse within 1 h of injection showed approximately 400,000 photons in the lung, ensuring a successful administration of cells (Fig. 6*A*). However, most cells were cleared from circulation within 24 h because photon counts were only a few hundreds (400–1,000) above the background (Fig. 6 *A* and *C*). In 5 wk, vehicle-treated PC3-Luc injected mice developed metastases in the lung, but almost 78% inhibition ($P < 0.05$) of metastasis was noted in the TFD_{100}-treated PC3-Luc injected mice (Fig. 6 *A* and *C*). Both vehicle and TFD_{100}-treated $gal3^{-/-}$ PC3-Luc injected mice showed negligible photons in the lungs (Fig. 6 *A* and *C*), suggesting a potential role of gal3 in the development of lung metastasis of PC3 cells. Micro metastases were evident in the lungs of the vehicle-treated PC3-Luc injected mice as visible by India ink staining (Fig. 6*D*). Moreover, lung sections of this group of mice showed enhanced proliferation of tumor cells as demonstrated by ki67 staining (Fig. 6*F* and Fig. S7*B*). The change in mouse body weight and serum chemistry related to the liver function for the treated group was unchanged compared with the vehicle group (Fig. S7*C* and Table S4), suggesting that TFD_{100} at experimental dose (50 μg per kg body weight) was not toxic to the animals.

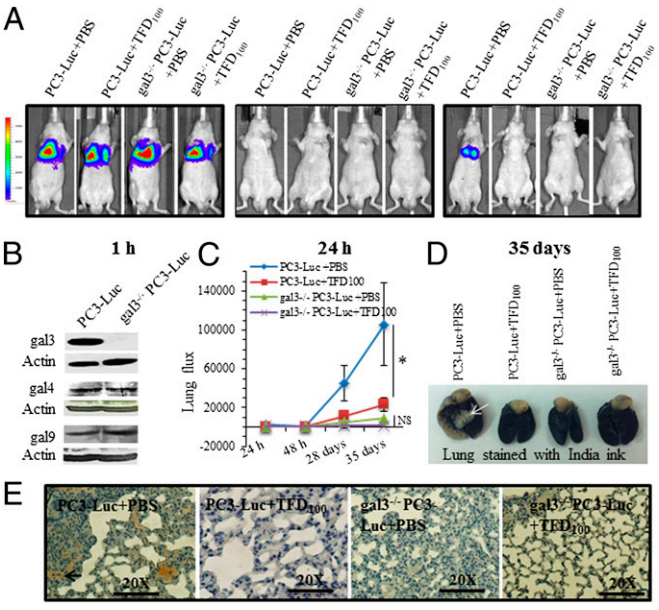

Fig. 6. Cancer metastasis induced by PC3 cells expressing a luciferase reporter (PC3-Luc) cells and its inhibition with TFD_{100}. (*A*) Representative images showing glowscale of luciferase-expressing PC3 cells (wild type or gal3 knockout) injected into the tail vein of nude mice. (*B*) Western blot showing expression of gal3, gal4, and gal9 in wild-type and $gal3^{-/-}$ (knockout) PC3-Luc cells. (*C*) Lung photon flux from untreated and TFD_{100}-treated mice. NS, not significant. (*D*) Lungs of PBS or TFD_{100}-treated mice stained with India ink. White arrow in the PC3-Luc+PBS injected mouse lung indicates tumor. (*E*) Representative diagrams showing ki67 stain of lung sections from untreated or TFD_{100}-treated mice.

Discussion

Cancer metastasis and immune suppression are critical issues in cancer therapy. Because tumor–endothelial cell interactions are considered a key step before cancer metastasis (1), disruption of such cell–cell interactions, may be an effective strategy for preventing metastasis. By antisense and knockout approaches, here we demonstrated that gal3 is involved in the promotion of angiogenesis, tumor–endothelial cell interactions, and metastasis of PCa in mice. These gal3-mediated functions can be disrupted by nanomolar levels of TFD_{100}, a TFD containing glycopeptide purified from cod AFGPs. However, a natural galectin-3 inhibitor (pectin) from citrus peel has been shown to inhibit tumor growth, angiogenesis, and metastasis of breast and colon cancers (17). Interestingly, a truncated gal3 (gal3C) also inhibited tumor growth and metastasis in orthotopic nude mouse model of human breast cancer (18).

TFD_{100} is very active (in picomolar range) in blocking gal3 binding to ligand as demonstrated by both solid phase assay and surface plasmon resonance analysis. The very strong affinity of TFD_{100} for gal3 can be explained as follows. The cod AFGPs are usually composed of several repeats of tripeptide of alanine-alanine-threonine in which the last residue is glycosidically linked to TFD (11). The TFD_{100} may also contain several repeats of tripeptide, which holds multiple TFD moieties. It is well established that multivalent ligands can enhance lectin binding, including that for gal3 (19) to a level far greater than the stoichiometric ratio—a phenomenon called "positive cooperativity" (20). In nude mice, picomole quantity of TFD_{100} inhibits PC3-induced metastasis and, thus, TFD_{100} may have application in the prevention of tumorigenesis. Because immune suppression is associated with chemotherapy of many cancers and gal3 promotes immune suppression by inducing apoptosis of cytotoxic T cells (9, 10), we investigated the efficacy of the TFD_{100} to block such T-cell apoptosis. Nanomolar TFD_{100} blocked gal3-mediated apoptosis of T cells, underscoring its importance in protecting antitumor response of the cytotoxic T cells. Furthermore, the protective effect of TFD_{100} on cytotoxic T cells suggests that the TFD_{100} can be used as an adjuvant in conjunction with the cancer drug.

Angiogenesis, the formation of new blood vessels from preexisting vasculature, is a key factor for not only normal homeostasis, but also in the pathogenesis of several diseases, including cancer (21). Angiogenic factors such as basic fibroblast growth factor (bFGF) and vascular endothelial growth factor (VEGF) families of cytokines activate endothelial cells and allow the cells to migrate, proliferate, and ultimately form a capillary lumen. Recent studies suggest that gal3 is involved in the promotion of angiogenesis through VEGF and bFGF (21). αvβ3 Integrin has also been demonstrated as a major gal3-binding glycoprotein, which is activated in a carbohydrate-dependent manner (21). Binding assays predict two gal3 receptors on HUVECs with nanomolar affinity ($K_d = 0.537 \times 10^{-9}$ and 7.161×10^{-9}), of which integrin may be one ligand (21). In this study, we have purified natural TFD_{100} with picomolar affinity to gal3 and also have demonstrated both in vitro and in vivo inhibition of angiogenesis with TFD_{100} (2–3.5 nM).

Among tumor-associated carbohydrate antigens, the TF antigen seems particularly a promising target for therapeutic strategy because of its outstanding tumor specificity (22). As an oncofetal antigen, TF antigen is cryptic in healthy adults, but is displayed on mucins and other membrane glycoproteins on tumor cells as a result of incomplete *O*-glycosylation (2, 22). In this study, we confirmed the presence of TF antigen in prostate carcinoma tissues, particularly in stage II and III (Fig. S3). For the past several years, the use of TF antigen as a cancer vaccine has been investigated by various groups and, in some cases, yielded promising results (22). The ability of the anti-TF antigen antibody to reduce tumorigenesis was also investigated. For example, treatment of mice with a monoclonal antibody to TF antigen alpha in vitro inhibited tumor–endothelial cell interactions, inhibited lung metastasis by at least 50%, and improved prognosis in a mouse breast cancer model (22). Overall, immunotherapeutic strategy targeted to TF antigen seems promising, but optimal response is still

needed for better results. Recent studies demonstrate that hematogeneous cancer metastases originate from intravascular growth of endothelium-attached cells highlighting the key role of tumor–endothelial cell interactions in cancer metastasis (1). A broad array of adhesion molecules, such as carbohydrates, lectins, cadherins, and integrins, participate at distinct stages in a multistep binding process of adhesion of tumor cells to the vascular endothelium (4). In an elegant study, Glinsky et al. (3) demonstrated that TF antigen present on the tumor cells caused gal3 mobilization and clustering on the endothelial surface before binding. We have demonstrated a strong expression of TF antigen in stage II–IV prostate tumor tissues (Fig. S3 *B* and *C*) supporting this hypothesis. In this study, we show that multiple receptors such as gal3, gal4, gal9, TF antigen, integrin, MUC1, and VEGFR1 participate in the adhesion of PC3 cells to HUVECs.

Immune suppression in the tumor microenvironment remains a major obstacle for the development of effective cancer immunotherapy (23). Recent studies show that regulatory T cells play a detrimental role in cancer immunotherapy because these cells accumulate in the tumor microenvironment and suppress immune responses (23). Tumor-associated galectins such as gal1 and gal3 contribute to tumor immune escapes by inhibiting the function of tumor-reactive T cells (9, 10). Particularly, a high dose of gal3 treatment abrogates the efficacy of tumor-reactive T cells and promotes tumor growth in a mouse tumor model (23). Cell surface glycoproteins such as CD29, CD7, CD95, CD98, and T-cell receptor have been shown to associate with gal3, which triggers the activation of an intracellular apoptotic signaling cascade followed by mitochondrial cytochrome *c* release and activation of caspase-3 (9). In this study, we have demonstrated gal3-mediated induction of apoptosis of MOLT-4, Jurkat, and activated $CD8^+$ $CD25^+$ T cells, which can be inhibited by nanomolar concentration of TFD_{100} (Fig. 5 and Fig. S6). Moreover, we have shown gal3 dose-dependent cell death of Jurkat and approximately 8% of cells die (measured by WST-1 stain) at 10 nM gal3, which is within the observed concentration of gal3 (0.2–1.0 μg/mL equivalent to 6.6–33 nM) in sera of patients with metastatic cancers including PCa (4). Thus, our results indicate that the pathological concentration of gal3 in cancer patient serum may be optimal for activated T-cell death. In fact, we have demonstrated here the apoptotic induction of activated $CD8^+CD25^+$ T cells by PCa patient sera and the inhibition of apoptosis with the TFD_{100}. Reduction of apoptosis by gal3-depleted patient serum further corroborates the participation of serum gal3 in the apoptotic induction of activated T cells. Furthermore, cancer cell (B16 melanoma used here as a model system)-associated gal3 induced apoptosis of tumor-specific activated $CD8^+CD25^+$ T cells (Fig. 5*J*). This result suggests that gal3-positive cancer cells may be able to evade immune system in vivo. Our overall results on gal3-mediated apoptosis of activated T cells and its inhibition with TFD_{100} underscore the effectiveness of TFD_{100} to protect antitumor immune response.

In nude mice, picomole quantity of TFD_{100} inhibits PC3-induced lung metastasis. It is clear from the data in Fig. 6 that PC3 metastasis is strongly suppressed either by treatment with TFD_{100} or by the RNAi-mediated depletion of gal3. Because the cells lacking gal3 (but not gal4 and gal9) could not form any significant metastases, TFD_{100} had no significant effect on them. If the gal3-deficient cells formed lung metastases, and TFD_{100} inhibited such metastases, it would be interpreted as TFD_{100}-mediated inhibition of metastasis occurred in a gal3-independent manner. Because no such observations were made and the differences between gal3-deficient cells and the corresponding TFD_{100} treatment are statistically not significant, it appears that gal3 is the primary target of inhibition by TFD_{100}.

The current report shows several unique aspects of TFD. From an edible source, we have purified TFD_{100} that possesses picomolar affinity to gal3. Because gal3 participates in many steps of metastasis and in immune suppression, the TFD_{100} may exert a "multipronged" attack on gal3-mediated tumorigenesis. The gal3–TFD interaction is a key factor driving metastasis in most epithelial cancers. Thus, a high-affinity inhibitor of such interactions like TFD_{100} should be a promising antimetastatic agent for the treatment of various cancers, including prostate adenocarcinoma.

Materials and Methods

Please see *SI Materials and Methods*. Work involving animals was approved by the Institutional Animal Care Committee of the University of Maryland. PCa patient sera were procured through the Cooperative Human Tissue Network (CHTN) of the National Cancer Institute (NCI). The Western Institutional Review Board (Olympia, WA) reviewed the protocol and determined that this study did not qualify as human subject research.

ACKNOWLEDGMENTS. We thank Dr. Mike Murphy (GE Healthcare Life Sciences) for conducting experiments on Biacore, Dr. Francesco Cappello (University of Palermo) for performing gal3 staining on prostate cancer tissues, and Dr. Hakon Leffler (Lund University) for providing gal4 and gal9 and their antibodies. The PC3-luciferase cell line was a kind gift from Dr. Patrick J. Casey (Duke University). This study was supported by the US Army Medical Research and Materiel Command Grant W81XWH-07-1-0565, the University of Maryland start-up fund, and in part by National Institutes of Health (NIH) Grants CA133935 and CA141970 (to H.A.) and GM070589 (to G.R.V.). E.K. is supported by a grant from The Council of Higher Education (Turkey). D.V.K. is supported by NIH Grant CA105005.

1. Al-Mehdi AB, et al. (2000) Intravascular origin of metastasis from the proliferation of endothelium-attached tumor cells: A new model for metastasis. *Nat Med* 6(1):100–102.
2. Yu LG (2007) The oncofetal Thomsen-Friedenreich carbohydrate antigen in cancer progression. *Glycoconj J* 24(8):411–420.
3. Glinsky VV, et al. (2001) The role of Thomsen-Friedenreich antigen in adhesion of human breast and prostate cancer cells to the endothelium. *Cancer Res* 61(12):4851–4857.
4. Yu LG, et al. (2007) Galectin-3 interaction with Thomsen-Friedenreich disaccharide on cancer-associated MUC1 causes increased cancer cell endothelial adhesion. *J Biol Chem* 282(1):773–781.
5. Zhao Q, et al. (2010) Interaction between circulating galectin-3 and cancer-associated MUC1 enhances tumour cell homotypic aggregation and prevents anoikis. *Mol Cancer* 9:154–165.
6. Shekhar MP, Nangia-Makker P, Tait L, Miller F, Raz A (2004) Alterations in galectin-3 expression and distribution correlate with breast cancer progression: Functional analysis of galectin-3 in breast epithelial-endothelial interactions. *Am J Pathol* 165(6):1931–1941.
7. Fukumori T, et al. (2006) Galectin-3 regulates mitochondrial stability and antiapoptotic function in response to anticancer drug in prostate cancer. *Cancer Res* 66(6):3114–3119.
8. Nangia-Makker P, Balan V, Raz A (2008) Regulation of tumor progression by extracellular galectin-3. *Cancer Microenviron* 1(1):43–51.
9. Hsu DK, Chen HY, Liu FT (2009) Galectin-3 regulates T-cell functions. *Immunol Rev* 230(1):114–127.
10. Li W, Jian-jun W, Xue-Feng Z, Feng Z (2010) CD133(+) human pulmonary adenocarcinoma cells induce apoptosis of CD8(+) T cells by highly expressed galectin-3. *Clin Invest Med* 33(1):E44–E53.
11. DeVries AL, Vandenheede J, Feeney RE (1971) Primary structure of freezing point-depressing glycoproteins. *J Biol Chem* 246(2):305–308.
12. Ideo H, Seko A, Yamashita K (2007) Recognition mechanism of galectin-4 for cholesterol 3-sulfate. *J Biol Chem* 282(29):21081–21089.
13. Nagae M, et al. (2006) Crystal structure of the galectin-9 N-terminal carbohydrate recognition domain from Mus musculus reveals the basic mechanism of carbohydrate recognition. *J Biol Chem* 281(47):35884–35893.
14. Pacis RA, et al. (2000) Decreased galectin-3 expression in prostate cancer. *Prostate* 44(2):118–123.
15. Ahmed H, Cappello F, Rodolico V, Vasta GR (2009) Evidence of heavy methylation in the galectin 3 promoter in early stages of prostate adenocarcinoma: Development and validation of a methylated marker for early diagnosis of prostate cancer. *Transl Oncol* 2(3):146–156.
16. Geng D, et al. (2010) Amplifying TLR-MyD88 signals within tumor-specific T cells enhances antitumor activity to suboptimal levels of weakly immunogenic tumor antigens. *Cancer Res* 70(19):7442–7454.
17. Nangia-Makker P, et al. (2002) Inhibition of human cancer cell growth and metastasis in nude mice by oral intake of modified citrus pectin. *J Natl Cancer Inst* 94(24):1854–1862.
18. John CM, Leffler H, Kahl-Knutsson B, Svensson I, Jarvis GA (2003) Truncated galectin-3 inhibits tumor growth and metastasis in orthotopic nude mouse model of human breast cancer. *Clin Cancer Res* 9(6):2374–2383.
19. Massa SM, Cooper DN, Leffler H, Barondes SH (1993) L-29, an endogenous lectin, binds to glycoconjugate ligands with positive cooperativity. *Biochemistry* 32(1):260–267.
20. Ketis NV, Girdlestone J, Grant CW (1980) Positive cooperativity in a (dissected) lectin-membrane glycoprotein binding event. *Proc Natl Acad Sci USA* 77(7):3788–3790.
21. Markowska AI, Liu FT, Panjwani N (2010) Galectin-3 is an important mediator of VEGF- and bFGF-mediated angiogenic response. *J Exp Med* 207(9):1981–1993.
22. Almogren A, et al. (2012) Anti-Thomsen-Friedenreich-Ag (anti-TF-Ag) potential for cancer therapy. *Front Biosci (Schol Ed)* 4:840–863.
23. Peng W, Wang HY, Miyahara Y, Peng G, Wang RF (2008) Tumor-associated galectin-3 modulates the function of tumor-reactive T cells. *Cancer Res* 68(17):7228–7236.